Cancer Chemother Pharmacol (2002) 50: 433–444
DOI 10.1007/s00280-002-0517-4

ORIGINAL ARTICLE

**Theodore F. Logan · Fayega Jadali · Merrill J. Egorin
Mark Mintun · Donald Sashin · William E. Gooding
Yong Choi · Harry Bishop · Donald L. Trump
Diane Gardner · John Kirkwood · Daniel Vlock
Candace Johnson**

Decreased tumor blood flow as measured by positron emission tomography in cancer patients treated with interleukin-1 and carboplatin on a phase I trial

Received: 19 September 2001 / Accepted: 21 August 2002 / Published online: 1 October 2002

Abstract *Background*: Positron emission tomography (PET) scanning can be used to measure blood flow. When interleukin-1α (IL-1) is given in a murine model, it induces acute hemorrhagic necrosis, tumor vascular injury and decreased tumor blood flow, and when given prior to carboplatin, there is enhanced antitumor activity compared to either agent alone. *Methods*: In a phase I trial of IL-1 and carboplatin, eligible patients with metastatic disease to the lung had PET scanning performed with ^{15}O water to assess tumor blood flow before and after IL-1 administration. Doses of IL-1 were 0.03, 0.06, 0.10, 0.15, 0.20 and 0.30 μg/kg given i.v. over 2 h. At 4 h after IL-1 initiation, carboplatin was administered as a 30-min i.v. infusion at a dose of 400 mg/m^2. Treatment was repeated every 28 days. Other measured parameters included granulocyte kinetics, integrin expression on circulating WBC, and carboplatin pharmacokinetics. Of 16 patients, 11 (8 evaluable) underwent PET scanning before and at 2, 4 and 24 h after IL-1 initiation. *Results*: Mean measured pretreatment tumor blood flow was 1.82 ml/min per g. At 2, 4 and 24 h it was 1.35, 1.67 and 1.62 ml/min per g respectively. Tumor blood flow was significantly decreased ($P < 0.008$) at 2 h after IL-1 initiation. In four patients, liver blood flow was measured at the same time-points as tumor blood flow. Liver blood flow was discordant with the tumor blood flow measures, showing no statistically significant change. IL-1 also caused a decreased WBC at 2 h after initiation ($n = 14$, $P = 0.025$).

This work was previously reported in part at the American Association for Cancer Research Annual Meeting 1994 and at the American Society of Clinical Oncology Meeting 1996.

T.F. Logan (✉) · M.J. Egorin · D.L. Trump
J. Kirkwood · D. Vlock
University of Pittsburgh, Pittsburgh, PA 15260, USA
E-mail: tlogan@iupui.edu
Tel.: +1-317-2743515

F. Jadali · D. Sashin · H. Bishop
Department of Radiology,
University of Pittsburgh Cancer Institute,
200 Lothrop Street, Pittsburgh, PA 15260, USA

M. Mintun
Mallinckrodt Institute of Radiology,
Division of Nuclear Medicine, St. Louis, MO 63110, USA

T.F. Logan · M.J. Egorin · D.L. Trump · D. Gardner
J. Kirkwood · D. Vlock
Department of Medicine, Division of Hematology-Oncology,
University of Pittsburgh Cancer Institute,
200 Lothrop Street, Pittsburgh, PA 15260, USA

W.E. Gooding
Department of Biostatistics,
University of Pittsburgh Cancer Institute,
200 Lothrop Street, Pittsburgh, PA 15260, USA

Y. Choi
Department of Nuclear Medicine,
Samsung Medical Center, Seoul, Korea

C. Johnson
Department of Pharmacology and Otolaryngology,
University of Pittsburgh Cancer Institute,
200 Lothrop Street, Pittsburgh, PA 15260, USA

T.F. Logan
Indiana University Cancer Center,
535 Barnhill Drive, RT 473, Indianapolis, IN 46202, USA

T.F. Logan
Current address: Department of Medicine,
Division of Hematology-Oncology,
Indiana University, Indianapolis, IN 46202, USA

D.L. Trump
Current address: Roswell Park Cancer Institute,
Buffalo, NY 14263, USA

C. Johnson
Current address: Roswell Park Cancer Institute,
Buffalo, NY 14263, USA

D. Vlock
Current address: Ethicon Endo-Surg,
Princeton, NJ 08540, USA

In addition, polymorphonuclear leukocyte (PMN) and monocyte surface expression of CD11b at 2 h was increased when measured by mean fluorescence intensity flow cytometry (PMN $P=0.0269$, monocytes $P=0.0420$). No consistent effect of IL-1 on either carboplatin AUC or platelet nadir was demonstrated. *Conclusions*: We conclude that IL-1 has measurable effects on tumor blood flow and causes a significant decrease in blood flow as measured by PET scanning with ^{15}O water at 2 h after initiation. This decrease is temporally associated with a significant leukopenia and an increased expression of the adhesion integrin CD11b on the circulating cell surface (PMN and monocytes). These results suggest that IL-1 causes decreased tumor blood flow in vivo in human cancer patients, an effect that was temporally related to cytokine-induced peripheral blood cellular changes. Furthermore, our findings suggest that PET scanning may be useful to assess the effect of a systemic antineoplastic agent on tumor blood flow in cancer patients.

Keywords Tumor blood flow · Interleukin-1 · Positron emission tomography scanning · Phase I trial · Carboplatin

Introduction

In the late 19th and early 20th centuries, William Coley observed that cancer patients treated with mixed bacterial vaccines (Coley's toxins) [11] experienced tumor necrosis. Currently, there is interest in the development of antiangiogenesis drugs to target tumor vasculature. The cytokines interleukin-1 (IL-1) and tumor necrosis factor (TNF) have been shown to induce tumor hemorrhagic necrosis in animal tumor models [5, 9]. In this process tumor vasculature collapses with bleeding into the necrotic tumor without affecting normal vasculature. The mechanism for hemorrhagic necrosis and the reasons that tumor vasculature seems to be targeted specifically are not well understood. Hemorrhagic necrosis has been well documented in animal models. Yet, since Coley's work nearly 100 years ago, it has not frequently been described in treated human cancer patients [45, 50] with the exception of TNF isolation-perfusion studies in melanoma [34] and sarcoma [18, 19]. The lack of human studies may be due to the absence, until now, of an established clinical method to evaluate changes in tumor blood flow or vascularization. Our study confirms that positron emission tomography (PET), which has been used to evaluate tumor glucose metabolism [57], and both organ [23, 37, 64] and tumor blood flow [2, 44, 60], can be used to evaluate changes in tumor blood flow with treatment.

Previous studies on animals at the University of Pittsburgh informed the approach we chose for human patients. IL-1 had been shown to induce hemorrhagic acute tumor necrosis with decreased tumor blood flow and increased tumor clonogenic cell kill [5]. Furthermore, IL-1 proved to potentiate the antitumor activity of various chemotherapeutic drugs (mitomycin C, puromycin, cisplatin, etoposide and carboplatin) [6, 10, 31, 32, 39, 54, 62]. The combination of IL-1 and carboplatin has been studied extensively in a murine tumor model, and these studies have demonstrated a significantly more enhanced clonogenic tumor cell kill when IL-1 is added to carboplatin than when either agent is used alone (3 logs of cell kill greater than carboplatin alone) [10]. The schedule and time sequence of IL-1 dosing is important: maximal tumor clonogenic cell kill is found when IL-1 is infused 4–6 h prior to carboplatin. The tumor and normal tissue content of platinum is significantly higher in animals treated with the combination of IL-1 and carboplatin compared to animals treated with either agent alone. Similar synergistic antitumor activity of IL-1/carboplatin has been noted by Wang et al. [58] in a human ovarian carcinoma xenograft model. However, in this model increased platinum uptake in tumors and increased DNA-platinum adduct formation in tumor cells was noted. The ability to alter tumor blood flow may impact significantly on the delivery of cytotoxic agents to the tumor microenvironment, yet the mechanism of the enhanced effect of IL-1 followed by carboplatin has not been explained nor has any potential relationship with altered tumor blood flow.

Phase I, early phase II, and other studies of IL-1 combined with cytotoxic drugs mainly to test its bone marrow-sparing effect, have been completed [15]. The pharmacokinetics of intravenous (i.v.) IL-1α have been incompletely described as serum samples in all but patients treated at the highest doses contained no measurable IL-1α in the phase I study [51]. Kopp et al. [33] have reported peak levels of IL-1α as 95 and 435 pg/ml in two patients treated with 1.0 μg/kg IL-1. These levels were undetectable within 1 h of completing infusion in both patients, and within 3 h in a third patient.

In our trial, a fixed dose of carboplatin was chosen and IL-1 was dose-escalated starting at a low dose described in a phase I trial of IL-1 alone [51]. We hypothesized that IL-1 would decrease tumor blood flow in human cancers in a similar fashion to that previously described in animals. We tested granulocyte kinetics and integrin expression, based on earlier human studies with TNF showing granulocyte and integrin changes at times when decreased blood flow and tumor hemorrhagic necrosis had been described in animal models [35, 36]. We hypothesized a relationship between these parameters and any IL-1-induced decrease in tumor blood flow.

Drawing from our animal investigations, we developed a new schedule of IL-1 followed by carboplatin for this phase I study and examined the effect of IL-1 on carboplatin pharmacokinetics and tumor blood flow as evaluated by PET scanning.

Methods

Patient selection

Patients eligible for this phase I trial had metastatic, progressive cancer without an established treatment option. They were entered and treated from July 1993 through July 1995. No chemotherapy or radiotherapy within the prior 4 weeks (8 weeks for mitomycin C or nitrosoureas) was permitted. An Eastern Cooperative Oncology Group (ECOG) performance status of ≤ 2 was required. Patients must have had measurable or evaluable disease, and no significant cardiac history. If female, a negative pregnancy test was mandatory. All patients were required to have a serum creatinine < 1.5 mg/dl or creatinine clearance > 60 ml/min, a serum bilirubin of < 2.0 mg/dl, and SGOT less than four times the upper limit of normal, a platelet count $> 100{,}000/\mu l$, a WBC count $> 3500/\mu l$ and normal prothrombin and partial thromboplastin times. To permit simultaneous PET imaging of the cardiac blood pool structures and tumor, patients who underwent PET scanning were required to have a metastatic lung tumor located within 10 cm (axially) of the left atrium or ventricle. Patients were ineligible if they had one or more CNS metastasis, leukemia, known hepatitis B surface antigen or human immunodeficiency virus positivity, or if their tumor was refractory to cisplatin or carboplatin (prior clinical disease progression on either agent). None of the patients had received prior platinum-based chemotherapy. This study was approved by the University of Pittsburgh IRB and all patients gave informed consent.

Treatment plan

IL-1 was given i.v. over 2 h. Carboplatin (400 mg/m^2) was infused i.v. over 30 min starting 4 h after initiation of the IL-1. Treatments were repeated every 28 days. PET scanning was performed on the first treatment day only in patients with appropriately localized metastatic tumor. Patients were treated for two cycles and re-evaluated for antitumor effect. All patients were followed for toxicity, which was graded according to the National Cancer Institute (NCI) Common Toxicity Criteria Scale. Hypotension was considered dose-limiting if it was not controlled with i.v. fluid or if treatment with vasopressors was required. Hypotension was treated with i.v. isotonic saline for blood pressure change with orthostatic maneuvers or supine hypotension. A pulse rise of ≥ 20 beats/min was treated with 250 ml of rapidly infused isotonic saline. A systolic or diastolic blood pressure decrease of ≥ 20 mmHg was treated with 500 ml of rapidly infused isotonic saline. Supine hypotension $< 90/60$ mmHg was treated with 1000 ml of rapidly infused isotonic saline. Intravenous fluid infusions were to be repeated every 20–30 min until blood pressure stabilized.

IL-1 was started at a dose of 0.03 μg/kg and escalated through the following dose levels: 0.06, 0.10, 0.15, 0.20, and 0.30 μg/kg. The carboplatin dose was held constant at 400 mg/m^2. Three patients were treated on each dose level. Patients with grade 3 toxicities, with the exception of hematologic, constitutional, stomatitis, and CNS, were taken off study. Dose modifications were allowed for grade 3 myelosuppression, CNS toxicity, nephrotoxicity, constitutional symptoms and hypotension. The maximum tolerated dose of this combination for a given dose level of IL-1 was defined as that level at which two of three patients experienced toxicity attributable to IL-1 of grade 3 or more.

Interleukin-1

IL-1α (IL-1) was provided by the National Cancer Institute Cancer Treatment Evaluation Program (NCI CTEP). Immunex Corporation (Seattle, Wash.) manufactured the IL-1 used for the first three patients on this protocol. Dainippon (Osaka, Japan) produced the IL-1 used to treat all subsequent patients. Both products were derived from *E. coli* and were 159 amino acid proteins differing by one amino acid in the second position. The molecular weights were similar and approximately 18,000 Da. Both proteins showed activity in different bioassays, which were not directly compared.

PET scanning

Subjects were imaged with an ECAT 951R/31 PET tomograph (CTI PET Systems, Knoxville, Tenn.), and 31 contiguous planes of data were recorded simultaneously over an axial length of 10.8 cm. Images were constructed using a 0.3 Hanning filter resulting in an average transverse spatial resolution of 12 mm (FWHM). Utilizing chest radiographs and/or CT images, subjects were positioned so that both the tumor and the heart were in the field of view of the tomograph. Preliminary rectilinear imaging using external rod sources of germanium (^{68}Ge) verified positioning. Before each pair of emission studies, 10 min of transmission data were acquired with the same rod sources for measured attenuation correction of the subsequent emission images. Prior to each set of scans, patients were positioned in the PET scan gantry based on transmission images compared to the first transmission image, and each positioning was confirmed by a physician so that the regions used were as close as possible across different time-points. Radioactive water was introduced as a 30-s peripheral i.v. infusion. Administered doses were in the range 25–50 mCi (925–1850 MBq) of $H_2{}^{15}O$. Data acquisition was initiated at the start of tracer injection.

The imaging protocol consisted of 12 time frames of 5 s each, followed by 5 of 10 s each, and 3 of 20 s each, for a total of 20 frames in 170 s. All frames were acquired in two dimensions. Before IL-1 infusion, two identical data sets, separated by 12 min, were acquired. Thereafter, similar pairs of data were acquired at 2, 4 and 24 h after the onset of the IL-1 infusion. Where two values were available, they were averaged; otherwise single values were used. Image data were acquired and analyzed using ECAT Scanner Software version 6.4d (CTI PET Systems, Knoxville, Tenn.) running on Sun SPARC stations.

For each pair of data, the corresponding transmission image as well as the CT images and the PET emission image summed over frames were used for region of interest (ROI) selection. Every attempt was made to place ROIs in the same place for the same tumor at each time-point in each patient. The left ventricular blood pool ROI was chosen to be small enough to minimize end systolic myocardial overlap. The lung tumor ROIs were chosen to include as much of the tumor as possible, while avoiding areas of possible necrosis as shown by greatly diminished tracer accumulation and corresponding decreased CT attenuation. These ROIs were drawn on multiple (three to seven) contiguous, transaxial image planes. The time sequence of radioactivity in these regions was then used to determine tumor blood flow.

The only treatment given for hypotension during PET scanning was i.v. normal saline which would not be expected to affect PET measurements.

Tumor blood flow determination

^{15}O-labeled water is a metabolically inert, freely diffusible tracer. Its behavior in tissue can be described by the following differential equation for a single tissue compartment model [28]:

$$dC_t(t)/dt = F \cdot C_a(t) - \left(F/V_d + \lambda\right) \cdot C_t(t)$$

where $C_t(t)$ is the regional tissue concentration of $H_2{}^{15}O$ [becquerels per milliliter (tissue)] as a function of time t, $C_a(t)$ is the arterial whole blood concentration of $H_2{}^{15}O$ (becquerels per milliliter) as a function of time t, F is the regional blood flow (milliliters of blood per milliliter of tissue per minute), V_d is the volume of distribution of water (milliliters of blood per milliliter of tissue), and λ is the decay constant of ^{15}O (0.338 min^{-1}).

The solution to this differential equation is given by [28]:

$$C_t(t) = F \cdot C_a(t) * \exp\left[-\left(F/V_d + \lambda\right) \cdot t\right]$$

where the asterisk denotes convolution. $C_t(t)$ represents the tissue response to an arterial input function $C_a(t)$. When $C_a(t)$ and $C_t(t)$ are measured over time with dynamic PET, estimates of both F and V_d can be obtained using standard nonlinear regression analysis.

In this study the left ventricular and tumor time-activity curves yielded the functions $C_a(t)$ and $C_t(t)$. The data were also fitted with an arterial blood volume component [27]:

$$C_t(t) = \mathrm{Vart} \cdot C_a(t) + F \cdot C_a(t) * \exp\left[-\left(F/V_d + \lambda\right) \cdot t\right]$$

where Vart is the arterial blood volume of the tumor. A zero value for this component suggests that the tumor arterial volume is negligibly small. Data could not be fitted unless the lung tumor time-activity curve rose later than the cardiac curve in all cases.

Carboplatin pharmacokinetics and pharmacodynamics

At 30 min and 1, 2, 8, and 24 h after initiation of the carboplatin infusion, blood was drawn into heparinized Vacutainers and separated by centrifugation at 1000 *g* for 10 min. The resulting plasma was transferred to 12×125-mm screw-capped polystyrene tubes and stored at –70°C. Protein-free plasma ultrafiltrates were prepared by placing a portion of plasma into Amicon Centrifree micropartition devices (Amicon Division, W.R. Grace and Co, Beverly, Mass.) and centrifuging the devices at 2000 *g* for 20 min at 4°C in a Sorvall RC-2B centrifuge (DuPont, Wilmington, De.).

The platinum concentrations in plasma and ultrafiltrates were determined with a Perkin-Elmer model 1100 flameless atomic absorption spectrometer (Perkin-Elmer, Norwalk, Ct.) using a previously described and validated assay [20]. Time courses of plasma concentrations of both total and ultrafilterable platinum in plasma were analyzed by non-compartmental methods. The area under the curve from zero to infinity (AUC) and terminal half-life ($t_{1/2}$) were estimated with the LaGrange function [63] as implemented by the LAGRAN computer program [46]. Carboplatin AUC was calculated from the relationship: carboplatin AUC = 1.90 (ultrafilterable platinum AUC). Carboplatin clearance was calculated from the definition: clearance = dose/AUC. The carboplatin AUC expected in each patient was calculated from the carboplatin dose delivered to that patient, that patient's creatinine clearance (Ccr) and a rearrangement of the Calvert dosing equation [7] in the form:

$$\text{AUC Expected} = \frac{\text{Carboplatin Dose (in mg)}}{(\mathrm{Ccr} + 25)}$$

For each patient, the measured ultrafilterable platinum AUC was used along with a sigmoid Emax model relating ultrafilterable AUC and percentage reduction in platelet count [3].

Blood counts and flow cytometry

CBC

Samples for complete blood counts (CBC) were drawn into standard ethylene-diaminetetraacetic acid vacuum tubes. Samples obtained from i.v. lines were used after discarding a dead volume, and, for all samples, either after interruption for the period of the blood sampling of any ongoing IL-1 infusion or from another i.v. site. Complete blood counts were performed using either a Coulter Counter S+IV (Coulter Electronics, Hialeah, Fl.) or a Coulter STKS system. Differential blood counts were performed manually or using the Coulter STKS system.

Integrins

At specified times, blood samples were collected in 4-ml heparinized tubes and immediately taken to the laboratory. Expression of $\beta 2$ integrins CD11a, b and c was determined by indirect immunofluorescence. A 100-µl sample of whole blood, containing approximately 1×10^6 cells was incubated on ice for 30 min with 20 µl monoclonal antibody to CD11a, b or c (AMAC, Westbrook, Me.). Cells were washed twice with cold phosphate-buffered saline (PBS) and resuspended in 100 µl PBS, 25 µl fetal bovine serum, and 5 µl FITC-labeled, goat, anti-mouse monoclonal antibody (Gam-FITC) (AMAC). The mixture was further incubated for 30 min on ice and in the dark. Following incubations, 2 ml lysing reagent (buffered ammonium chloride, pH 7.4) was added, and the specimen was immediately agitated vigorously. The sample was then fixed with 200 µl 2% paraformaldehyde. Analysis was performed with a FACScan (Becton Dickinson, Mountain View, Calif.) operated at a wavelength of 488 nm. Background fluorescence was determined using an appropriate immunoglobulin isotype subclass control that was run with each specimen. Cells for analysis were selected from cytograms on the basis of forward and right-angle light scatter characteristics. The fluorescence intensity of the appropriately gated cells was measured, and the mean fluorescence intensity was determined as the mean channel number of the fluorescence intensity peak.

Statistics

Within-patient differences at each time were calculated by subtracting the patient's baseline value. A two-tailed signed-ranks test was then applied to the set of differences at each time-point. Linear regression and correlation were used to examine associations between clinical and pharmacokinetic parameters. Residuals from regression models were plotted and examined for appropriateness of the models.

Results

Tumor blood flow measurements by PET

Of 16 patients (Table 1), 11 underwent PET scanning. Evaluable information was obtained in eight (five metastatic renal cell carcinomas, one metastatic thyroid carcinoma, and two metastatic breast carcinoma). In one patient, no data were obtained, possibly secondary to necrotic tumor. In another patient, the delay between $H_2{}^{15}O$ injection and imaging was prolonged due to technical difficulties, and the data were not usable. In a third patient, the data could not be properly modeled.

Table 1 Patient characteristics

Male/female	10/6
Age (years)	
Median	60.5
Range	40–77
Performance status	
0	12
1	2
2	2
Tumor type	
Renal cell	7
Breast	2
Colon/rectum	4
Lung	1
Thyroid	1
Melanoma	1
Prior therapy	
Surgery	15
Chemotherapy	14
Radiotherapy	8
Immunotherapy	2
Hormone therapy	1

After injection of $H_2{}^{15}O$, time-activity curves were generated from PET count measurements within ROIs placed over the heart and the tumor (Fig. 1). These curves allowed calculation of tumor blood flow, volume of distribution, and blood volume for the tumor as described in the model presented (Tables 2, 3 and 4). Decreased tumor blood flow was noted in all eight patients at 2 h after IL-1 initiation ($P=0.008$; Table 5 and Fig. 2A). At 4 and 24 h, tumor blood flow increased relative to the value at 2 h and was no longer significantly different from baseline ($P=0.25$ at 4 h, $P=0.84$ at 24 h). Because patients receiving IL-1 became hypotensive (Fig. 3), this decrease in systemic blood pressure could theoretically account for the observed reduction in tumor blood flow. However, the lowest value for tumor blood flow occurred at 2 h while systemic blood pressure rose early and then gradually decreased reaching a nadir at 4–6 h, suggesting that systemic hypotension may not be solely responsible for these time-dependent changes. Liver and tumor blood flow was measured simultaneously in four patients, and in three of the four liver flow rose when tumor flow was maximally decreased (Fig. 2B). Additionally, the time-activity curves from normal liver were different in shape (not shown) from those from metastatic lung nodules.

The volume of distribution of $H_2{}^{15}O$, which when described by this method estimates the volume of tissue perfused, was noted to be in a similar range to that previously found in primary breast cancers [60]. It decreased significantly at 2 h after IL-1 initiation ($P=0.008$, signed ranks test) and subsequently increased toward baseline. Conversely, tumor blood volume increased at both 2 and 4 h after IL-1 initiation ($P=0.03$, signed ranks test). Changes in these parameters are related. Both flow and volume of distribution decline and rise together in time while tumor blood volume increases.

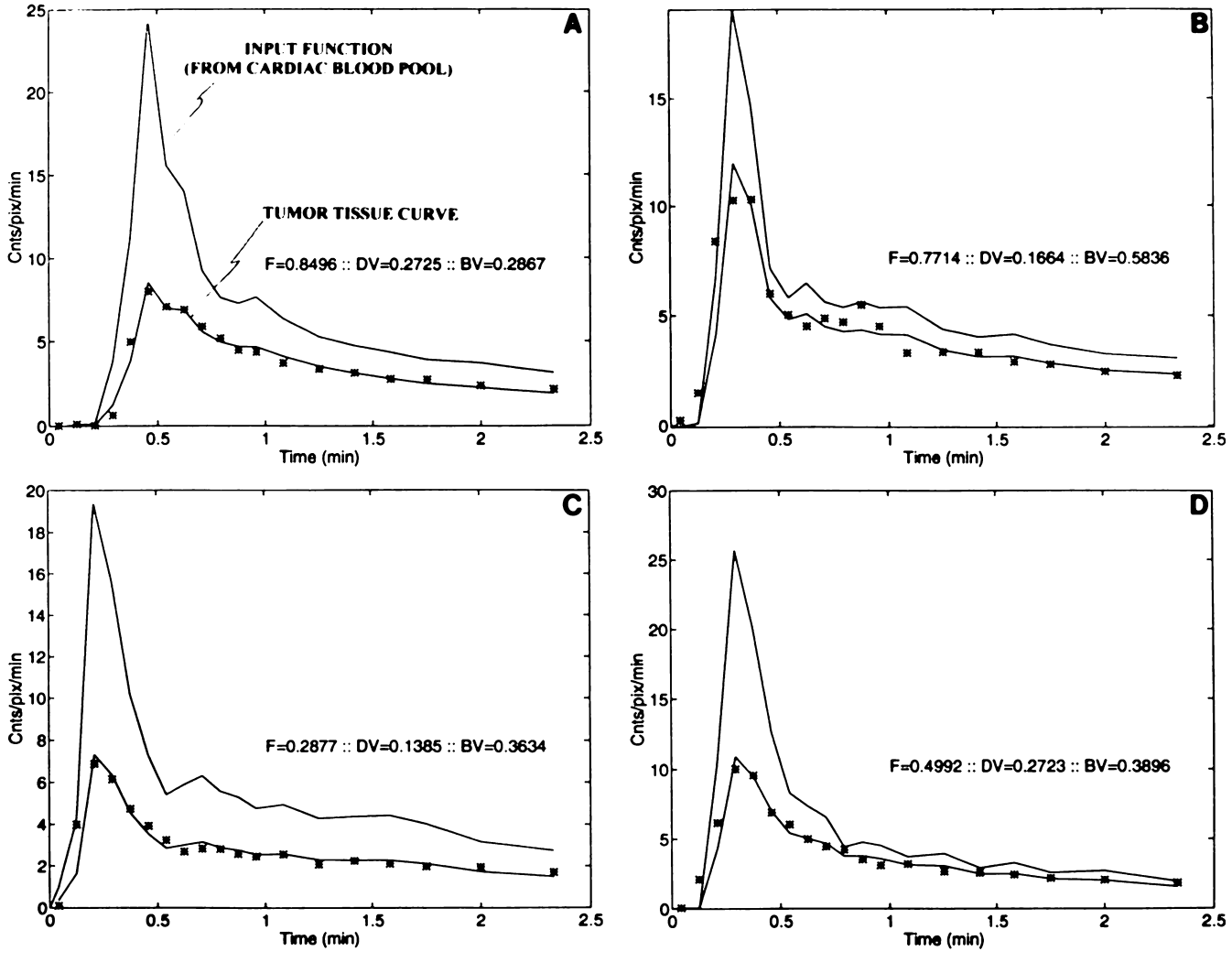

Fig. 1A–D Time activity curves obtained from ROIs drawn over heart and tumor PET scan images after rapid injection of $H_2{}^{15}O$. Representative example from a patient at times: **A** pre-IL-1, **B** 2 h, **C** 4 h, **D** 24 h (*F* tumor blood flow, *DV* volume of distribution, *BV* blood volume, *cnts/pix/min* counts/pixel/minute). Curves were drawn to fit the data as described in the text. These data were obtained from the second patient (no. 307) enrolled who had renal cell cancer and was treated on the lowest dose level

Table 2 Tumor blood flow (milliliters per minute per gram)

Patient ID	Pretreatment	After IL-1 initiation		
		2 h	4 h	24 h
233 (RCC)	1.90	1.66	3.07	2.10
307 (RCC)	0.72	0.47	0.51	0.57
345 (RCC)	3.44	2.39	3.22	3.30
640 (RCC)	1.08	1.00	1.21	1.34
669 (breast)	0.85	0.74	0.75	0.72
776 (thyroid)	3.20	1.92	1.86	2.13
789 (RCC)	1.57	1.38	1.27	1.63
796 (breast)	1.81	1.24	1.44	0.70
Mean ± SE	1.82 ± 0.36	1.35 ± 0.22*	1.67 ± 0.35	1.56 ± 0.33

*$P < 0.01$

Pretreatment tumor blood flow was greater than previously described [60] and was highest in patients with renal cell and thyroid cancer metastases.

White blood cell and integrin kinetics

In 14 patients, serial WBC counts were obtained and the surface expression of CD11a, b and c on granulocytes, monocytes, and lymphocytes was measured. A substantial decrease in WBC count occurred 2 h after IL-1 initiation ($n = 14$, $P = 0.025$). At this time, levels of granulocytes ($P = 0.027$), monocytes ($P = 0.042$), and ymphocytes were significantly diminished. Subsequently, there was a recovery and overshoot with increasing numbers of granulocytes and monocytes present in the peripheral blood (Fig. 4A, B). Serial measurements of CD11a, b and c on granulocytes, monocytes, and lymphocytes in 14 patients at the same time-points demonstrated increased expression of cell surface CD11b, expressed as mean fluorescence intensity, on both granulocytes ($P = 0.0269$) and monocytes ($P = 0.0420$) at 2 h (Fig. 4C, D). There

Table 3 Volume of distribution (milliliters per milliliter)

Patient ID	Pretreatment	After IL-1 initiation		
		2 h	4 h	24 h
233 (RCC)	0.6247	0.5676	0.6369	0.6589
307 (RCC)	0.3769	0.3209	0.2468	0.3025
345 (RCC)	0.8965	0.8255	0.8100	0.6475
640 (RCC)	0.5676	0.5150	0.5908	0.5955
669 (breast)	0.5020	0.4725	0.4882	0.53047
776 (thyroid)	0.7669	0.7474	0.7716	0.6530
789 (RCC)	0.3149	0.2716	0.3421	0.3618
796 (breast)	0.4107	0.3490	0.2584	0.4143
Mean ± SE	0.5575 ± 0.07	0.5086 ± 0.07*	0.5180 ± 0.08	0.5200 ± 0.05

*$P < 0.01$

Table 4 Tumor blood volume (per milliliter)

Patient ID	Pretreatment	After IL-1 initiation		
		2 h	4 h	24 h
233 (RCC)	0.0394	0.1040	0.0600	0.0170
307 (RCC)	0.2150	0.3874	0.3604	0.3805
345 (RCC)	1.00×10^{-9}	1.00×10^{-9}	1.0×10^{-9}	1.00×10^{-9}
640 (RCC)	0.0386	0.1372	0.1124	0.0560
669 (breast)	0.1780	0.2440	0.3117	0.3510
776 (thyroid)	0.0077	0.00652	1.00×10^{-9}	1.00×10^{-9}
789 (RCC)	0.2660	0.3129	0.3672	0.2227
796 (breast)	0.04939	0.1916	0.2424	0.1075
Mean ± SE	0.0990 ± 0.04	0.1730 ± 0.05**	0.1820 ± 0.06**	0.1420 ± 0.06

**$P < 0.05$

Table 5 Tumor blood flow/liver blood flow by time

	Tumor				Liver			
	Pre-IL-1	2 h	4 h	24 h	Pre-IL-1	2 h	4 h	24 h
Number of patients	8	8	8	8	4	4	4	2
Blood flow (ml/min/g, mean ± SD)	1.82 ± 1.02	1.35 ± 0.64	1.67 ± 1.00	1.62 ± 0.88	0.74 ± 0.50	0.78 ± 0.12	1.00 ± 0.42	0.60 ± 0.07
P value[a]	–	0.008	0.250	0.844	–	0.875	0.265	–

[a]Signed ranks test vs pre-IL-1

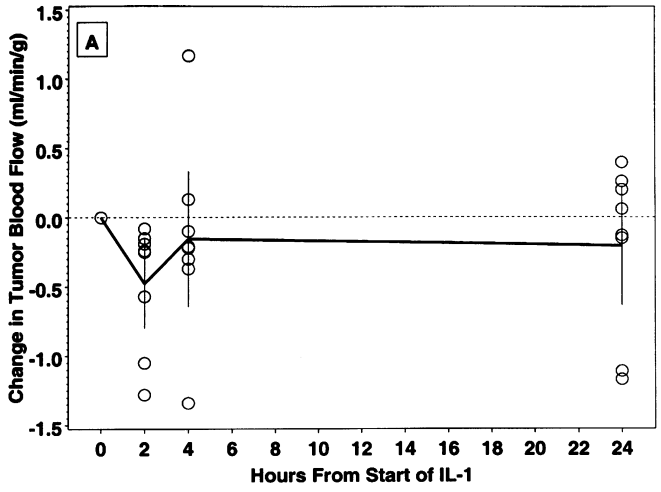

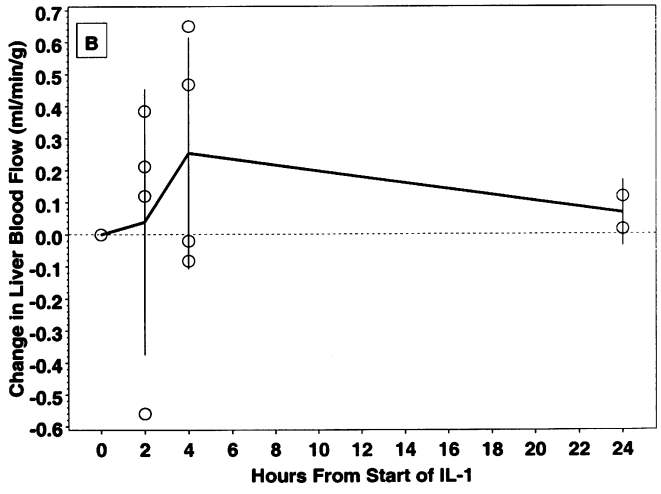

Fig. 2 **A** Posttreatment within-patient changes in tumor blood flow measured by PET pre-IL-1, and at 2, 4 and 24 h after the start of IL-1. Each point indicates the difference between the posttreatment tumor blood flow and the baseline. Means at each time are connected and error bars are drawn to depict two standard errors. Tumor blood flow at 2 h was significantly lower than at pretreatment (signed ranks test $P=0.008$). **B** Posttreatment within-patient changes in liver blood flow measured by PET pre-IL-1, and at 2, 4 and 24 h after the start of IL-1. Each point indicates the difference between the posttreatment mean liver blood flow and the baseline. Means at each time are connected and error bars are drawn to depict two standard errors. Measurements were available for four patients

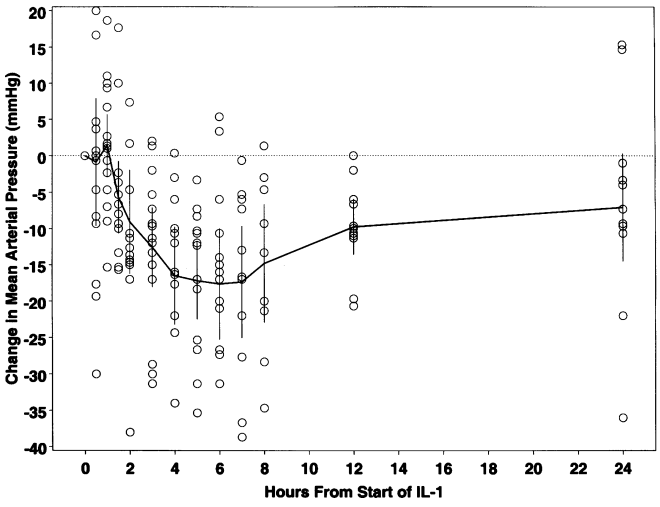

Fig. 3 Posttreatment within-patient changes in mean arterial pressure during the 24 h after the start of IL-1 infusion. Each point indicates the difference between the posttreatment arterial pressure and the baseline. Means at each time are connected and error bars are drawn to depict two standard errors. Mean arterial pressure was significantly diminished at 3 through 12 h (all signed ranks tests $P<0.05$)

were no significant changes in CD11a and c (data not shown).

Carboplatin pharmacokinetics/pharmacodynamics

Carboplatin pharmacokinetics were measured in ten patients. The correlation coefficient for predicted AUC of carboplatin versus observed AUC of carboplatin was 0.77 ($P=0.02$) suggesting no significant difference. In Fig. 5A, the difference between the observed AUC and that predicted by the Calvert formula [7] and IL-1 dose is plotted. The regression slope was not different from zero ($P=0.38$) suggesting that IL-1 dose could not explain any deviation in carboplatin AUC from that predicted. Increasing IL-1 dose had no effect on observed carboplatin AUC ($P=0.46$). The percentage decrease in platelet count [(pretreatment platelet count–posttreatment platelet count)/pretreatment platelet count×100] versus IL-1 dose is plotted in Fig. 5B. The regression slope of –278 ($P=0.02$) is equivalent to a 2.78% decrease in platelets for an increase of 0.01 μg/kg of IL-1, and suggests that IL-1 might modulate thrombocytopenia. However, an alternate analysis of percentage error yielded a mean percentage error of –4%, which is not significantly different from zero. This latter result implies no effect of IL-1 dose on platelet count.

Clinical outcome

A total of 16 patients (Table 1) were entered into the trial, and the maximum tolerated dose was never reached. The trial was stopped because IL-1 became unavailable for clinical use. Seven patients had stable disease after two cycles of therapy. Interestingly, one patient with heavily pretreated renal cell cancer had gradual tumor shrinkage by 51% over ten cycles of treatment. CT scans were not obtained at 1 month after tumor shrinkage had reached 50% so that the 1-month duration required in the definition of partial response was not met. Therefore, the patient was considered to have stable disease. This patient subsequently progressed with an intramedullary spinal cord metastasis.

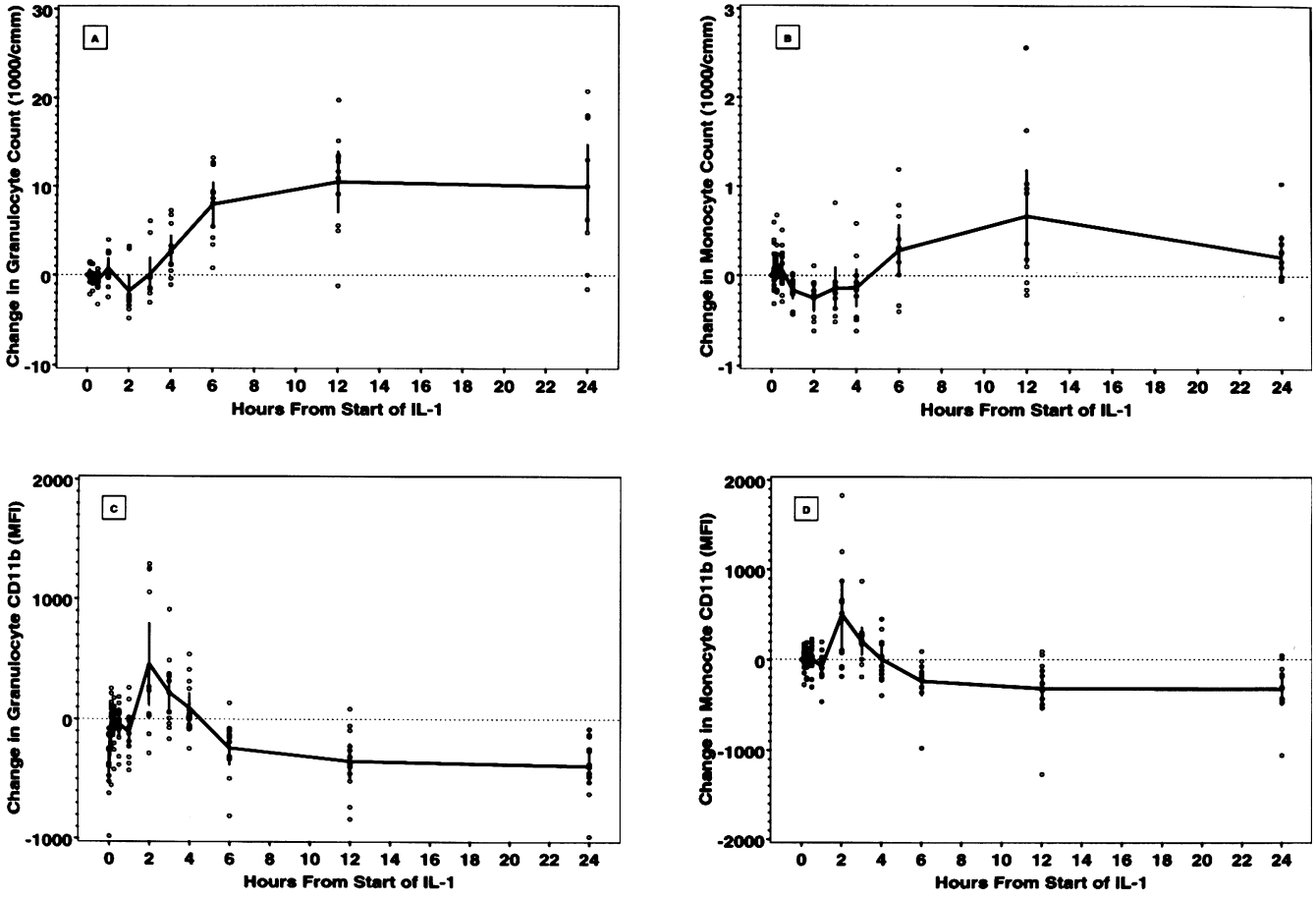

Fig. 4A–D Posttreatment within-patient changes in granulocytes, monocytes, and CD11b expression on granulocytes and monocytes (**A**, **B**, **C**, and **D**, respectively). Each point indicates the difference between the posttreatment measurement and the baseline (*MFI* mean fluorescence intensity). Means at each time are connected and error bars are drawn to depict two standard errors. The plots show the inverse relationship between counts of granulocytes and monocytes and contemporaneous surface marker expression of the adhesion molecule CD11b

Toxicity

Toxicities encountered in this trial were primarily constitutional and hematologic (Table 6). Hypotension was prominent, but readily treated by rapid i.v. fluid boluses of crystalloid solution. No patient required pressors. Because IL-1 became unavailable, only one patient was treated with the maximum dose of 0.3 μg/kg, which was the maximum tolerated dose in other trials of IL-1 given by daily dosing for up to 7 days.

Dose effects

In this small data set, there was no significant effect of IL-1 dose on grade 3-4 toxicity (Cochran Armitage trend test), change in tumor blood flow at 2 h by PET (both Jonckheere's test for trend $P=0.8$, and Kruskal Wallis test for equality $P=0.94$) or grade of hypotension (Jonckheere's two-tailed exact test $P=0.41$ and exact chi squared two-tailed $P=0.48$). Usable tumor blood flow measurements came from patients on the 0.03, 0.06 and 0.1 μg/kg dose levels.

Discussion

We showed that IL-1 decreased blood flow in metastatic lung tumor nodules in patients with cancer. This decrease occurred within 2 h of IL-1 initiation and was quickly, but partially, reversible. The volume of distribution which reflects the volume of tissue perfused followed the same pattern as tumor blood flow with significant reductions at 2 h, then partial recovery. The tumor blood volume was significantly increased by approximately 75% at 2–4 h. One possible explanation for these findings would be a transient hemorrhagic necrotic-like effect in tumor nodules reflected in both decreased tumor blood flow and volume of distribution and increased blood volume (secondary to an element of hemorrhage into the tumor). The time-course of decreased blood flow was similar to that observed during IL-1-mediated hemorrhagic necrosis in animal tumor models [5, 12]. There was no dose effect of IL-1 observed on tumor blood flow; however, we believe the sample size was too small to exclude such an effect.

Tumor blood flow dropped at 2 h after IL-1 initiation by approximately 25% and volume of distribution

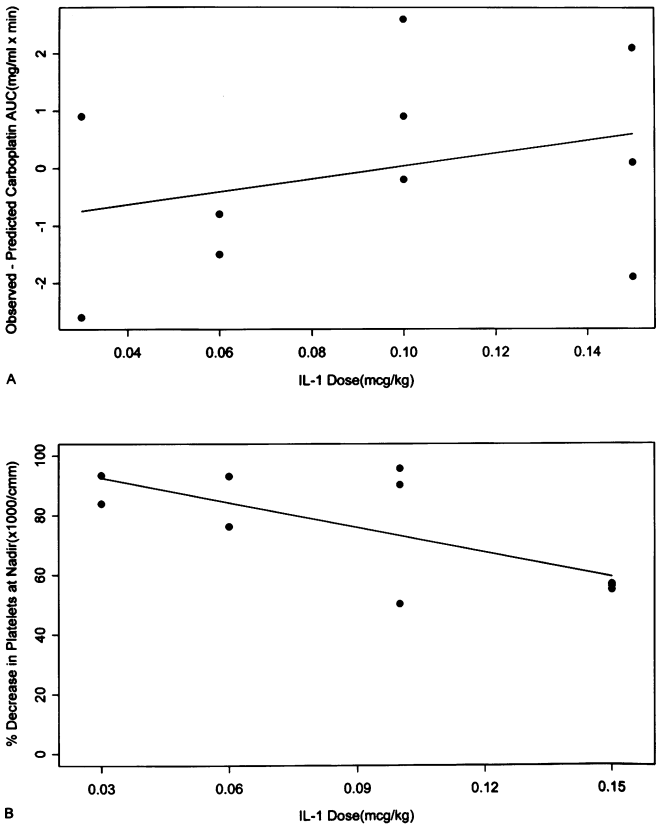

Fig. 5 **A** Excess carboplatin AUC (mg/ml·min) by IL-1 dose (μg/kg). The excess carboplatin AUC is the difference between the observed AUC and that predicted by the Calvert formula from the patient's creatinine clearance. The estimated regression slope is not significantly different from zero ($P=0.3851$) suggesting that IL-1 dose could not explain any deviation between actual carboplatin AUC and AUC predicted by the Calvert formula. **B** Percentage decrease in the platelets at nadir following the first course of 400 mg/m^2 carboplatin vs dose of IL-1 (μg/kg) given 4 h before the carboplatin. The estimated regression slope of –278 ($P=0.0234$) suggests that IL-1 may mitigate thrombocytopenia

Table 6 Treatment-related toxicity (highest grade of toxicity per patient where toxicities were rated either possibly or probably related to treatment)

	Grade 3	Grade 4
Hematologic		
Thrombocytopenia	3	8
Leukopenia	6	
Anemia	5	
Nausea	1	
Vomiting	2	
Weight loss	1	

dropped by 9% at the same time, suggesting two possible effects of IL-1 on tumor vasculature. The decrease in volume of distribution may indicate decreased tissue perfusion secondary to disruption of the vasculature as has been described during hemorrhagic necrosis. Whereas the remaining blood flow reduction may reflect reduced capillary blood flow or shutting down of capillary beds in a manner which would not effect tissue perfusion. We speculate that this latter effect may prove transient and might possibly be related to the release of endogenous vasoconstrictive factors such as endothelin-1 under the influence of IL-1 [26], or of other factors such as endogenous angiostatin [53].

In clinical trials with IL-1, there have been a small number of clinical responses [15]. Because clinical response is determined by CT scanning or other anatomically based radiologic techniques, it is possible that subclinical reduction in tumor blood flow with hemorrhagic necrosis may have occurred following IL-1 administration, but was not detectable. The mechanism of this decrease in tumor blood flow is not known, but it is noteworthy that the decrease in peripheral blood granulocytes and monocytes associated with IL-1 treatment was most pronounced at 2 h, coincident with the time of maximal decreased tumor blood flow. Both cell types had increased expression of the adhesion protein CD11b on their surface at this time. As we have previously postulated [35, 36], the WBC kinetic patterns that have been described with a related cytokine, TNF, indicate that granulocytes and monocytes are leaving the peripheral circulation. Increased cell surface expression of CD11b suggests that these cells may be adhering to vascular endothelium through this integrin, as has been shown in vitro [24] and in vivo [8]. It is also possible that, following IL-1 administration, granulocytes and monocytes adhere to tumor vascular endothelium, thereby reducing tumor blood flow and, under the influence of IL-1, initiating a hemorrhagic necrotic response. However, there are scant data in animal models [16, 25] or humans as to the mechanistic involvement of WBC in the induction of hemorrhagic necrosis. In a study of melanoma and sarcoma patients undergoing isolation perfusion therapy with high-dose TNF, interferon gamma and melphalan, a massive polymorphonuclear cell infiltrate was noted in tumor biopsy specimens as early as 2 to 3 h after completion of the TNF [43]. In addition, responding tumors pathologically demonstrate hemorrhagic necrosis following treatment [43].

PET scanning has been used in cancer patients mainly for tumor glucose metabolism imaging. Other applications for PET scanning are also possible. These include tumor receptor-binding assays, measurement of uptake of labeled chemotherapeutic agents, amino acids and amino acid analogs and measurement of rates of DNA synthesis with labeled thymidine as well as measurement of tumor blood flow and hypoxia [41, 57]. Tumor blood flow can be measured using i.v. $H_2{}^{15}O$ or inhaled $C^{15}O_2$ [2, 29, 57]. Other tracers, such as ^{82}Rb and ^{62}Cu, have also been used in preliminary studies for tumor blood flow imaging.

Tumor blood flow has been measured by PET in patients with primary breast carcinoma [2, 60] and glioma [44]. Wilson et al. [60] using a similar method with ^{15}O-labeled water found a mean tumor blood flow of 0.29 ml/min per g in 20 primary breast cancers. Our mean pre-IL-1 tumor blood flow result was substantially higher (1.82 ml/min per g), but this may reflect

differences between tumor type (relatively avascular breast carcinoma vs relatively hypervascular renal cell carcinoma) or differences between primary and metastatic cancers. The important measurements were the relative changes noted from baseline. The absolute blood flow measurements are subject to inaccuracy due to partial volume effect or spill-over. Increased tumor blood flow is not likely to reflect vascular input from the pulmonary artery since cardiac time activity curves had to rise before lung tumor time activity curves for the data to be properly fitted.

Liver blood flow comprises both hepatic artery and portal vein flow. Ziegler et al. [64] have recently evaluated liver blood flow using ^{15}O-labeled water and dynamic PET scanning compared to microsphere injection in foxhounds, and suggest that data obtained using a standard one-compartment blood flow model would be a good approximation of liver blood flow. In order to determine whether blood flow in normal tissues is affected by IL-1, PET images of normal liver were obtained in four patients. Normal liver blood flow was not decreased in this small sample. The discordance with tumor blood flow could be explained by a direct effect of IL-1 on tumor vasculature or, conversely, an effect to increase liver blood flow directly through a shunting mechanism (as occurs in septic shock) or through increased liver production of nitric oxide. In this study, we are not suggesting that we measured absolute liver blood flow, but rather relative liver blood flow compared to pretreatment.

It has been suggested that tumor blood flow may be modified for therapeutic gain [30, 38, 47]. PET scanning has been used in one study to evaluate the effect of radiosurgery on regional cerebral blood flow in patients with meningiomas or metastases [59]. To our knowledge, our study is one of the first in which the effect of a systemically administered drug or cytokine on tumor blood flow has been measured in vivo in cancer patients. As there are agents (such as IL-1 [15, 55], TNF [34], flavone acetic acid [14], CM101 [17], KB-R8498 [49], antibodies targeting tumor vessels [42], and antiangiogenic drugs [22]) that reportedly have effects on tumor vasculature and tumor blood flow, this technique may become a way to evaluate and quantify any such vascular effect. In fact our study is a relatively old study (patient accrual stopped in 1995), and more recently several groups have published studies in which PET was used to measure tumor blood flow and the effects of novel therapies on it in cancer patients [1, 21, 48].

In prior clinical studies with IL-1, hypotension was a dose-limiting toxicity [15]. In most of these studies, IL-1 was given at a dose of up to 0.3 μg/kg by short i.v. infusion daily for up to 7 days with dose-limiting toxicity being hypotension [15]. In one study, pressor support was required at IL-1 doses ≥0.3 μg/kg [51]. Prominent effects of IL-1 on the peripheral leukocyte populations have been reported as has a possible platelet-sparing effect [15]. IL-1 was subsequently given in combination with single agents such as 5-FU [13], carboplatin [52, 56] or combined chemotherapy [4, 40, 61] in an attempt to demonstrate a marrow-protective effect. Such an effect is suggested in a study by Smith et al. [52] and, in addition, five patients, including a patient with renal cell carcinoma, had a partial clinical response.

Our phase I trial delivered high doses of IL-1. While hypotension was a significant finding in our study, it was manageable with i.v. crystalloid solution only. No patient in our trial required pressors. The maximum tolerated dose of this combination was not reached. All other toxicities in this trial were expected.

In this small series, we were unable to demonstrate a consistent effect of IL-1 on either carboplatin AUC or platelet nadir. Some in vivo interaction may occur because animal data have shown increased platinum concentrations in tumor after combined treatment with carboplatin and IL-1 [10, 58].

We were able to demonstrate a measurable decrease in tumor blood flow after systemic IL-1 as measured by PET, which standard radiographic techniques based on anatomy would be unable to detect. As noted above, there are many new (and some old) anticancer agents that target tumor vasculature. Current radiographic techniques do not allow an assessment of the antivascular effect of these agents. As our study demonstrated, $H^{15}O_2$ PET scanning is a technique that could be used to assess antivascular effects by measuring tumor blood flow before and after treatment. It would then be possible to evaluate new antivascular agents for their antivascular effect in cancer patients.

Acknowledgements We thank the house staff of the University of Pittsburgh, Department of Medicine, and the nursing and support staff of unit 8 south Montefiore-University Hospital, the General Clinical Research Unit and of the University of Pittsburgh PET Facility for excellent care of the patients. We thank David Townsend PhD for helpful comments. We also thank Langdon L. Miller MD, Terry Jones PhD, Jeffrey T. Yap PhD and Michael Wong MD for valuable input. T.F.L. was supported in part by an American Cancer Society Clinical Oncology Career Development Award. We thank Ms. Marcia Schmitz and Ms. Alisa Reese for their excellent secretarial support.

References

1. Bacharach SL, Libutti SK, Carrasquillo JA (2000) Measuring tumor blood flow with H(2)(15)O: practical considerations. Nucl Med Biol 27:671
2. Beaney RP, Lammertsma AA, Jones T, McKenzie C G, Halnan KE (1984) Positron emission tomography for in-vivo measurement of regional blood flow, oxygen utilisation, and blood volume in patients with breast carcinoma. Lancet 1:131
3. Belani CP, Kearns CM, Zuhowski EG, Erkmen K, Hiponia D, Zacharski D, Engstrom C, Ramanathan RK, Capozzoli MJ, Aisner J, Egorin MJ (1999) A phase I trial, including pharmacokinetic and pharmacodynamic correlations, of combination paclitaxel and carboplatin in patients with metastatic non-small cell lung cancer. J Clin Oncol 17:676
4. Bookman MA, Caron DA, Hogan WH, Kilpatrick D, Rosenblum N, Schider RJ, Ozols RF (1993) Phase-I evaluation of dose-intense chemotherapy with interluekin-1α (IL-1α) for gynecologic malignancies. Proc Am Soc Clin Oncol 12:868

5. Braunschweiger PG, Johnson CS, Kumar N, Ord V, Furmanski P (1988) Antitumor effects of recombinant human interleukin-1α in RIF-1 and Panc 02 solid tumors. Cancer Res 48:6011
6. Braunschweiger PG, Jones SA, Johnson CS, Furmanski P (1991) Potentiation of mitomycin C and porfiromycin antitumor activity in solid tumor models by recombinant human interleukin-1α. Cancer Res 51:5454
7. Calvert AH, Newell DR, Gumbrell LA, O'Reilly S, Burnell M, Boxall FE, Siddik ZH, Judson IR, Gore ME, Wiltshaw E (1989) Carboplatin dosage: prospective evaluation of a simple formula based on renal function. J Clin Oncol 7:1748
8. Carlos TM, Harlan JM (1994) Leukocyte-endothelial adhesion molecules. Blood 84:2068
9. Carswell EA, Old LJ, Kassel RL, Green S, Fiore N, Williamson B (1975) An endotoxin-induced serum factor that causes necrosis of tumors. Proc Natl Acad Sci U S A 72:3666
10. Chang MJ, Yu WD, Reyno LM, Modzelewski RA, Egorin MJ, Erkmen K, Vlock DR, Furmanski P, Johnson CS (1994) Potentiation by interleukin 1α of cisplatin and carboplatin antitumor activity: schedule-dependent and pharmacokinetic effects in the RIF-1 tumor model. Cancer Res 54:5380
11. Coley WB (1894) The treatment of inoperable malignant tumors with toxins of erysipelas and the *Bacillus prodigiosus*. Am J Med Sci 108:50
12. Constantinidis I, Braunschweiger PG, Wehrle JP, Kumar N, Johnson CS, Furmanski P, Glickson JD (1989) ^{31}P-nuclear magnetic resonance studies of the effect of recombinant human interleukin-1α on the bioenergetics of RIF-1 tumors. Cancer Res 49:6379
13. Crown J, Jakubowski A, Kemeny N, Gordon M, Gasparetto C, Wong G, Sheridan C, Toner G, Meisenber GB, Botet JA (1991) Phase I trial of recombinant human interleukin-1α alone and in combination with myelosuppressive doses of 5-fluorouracil in patients with gastrointestinal cancer. Blood 78:1420
14. Cummings J, Smyth JF (1989) Flavone 8-acetic acid: our current understanding of its mechanisms of action in solid tumours. Cancer Chemother Pharmacol 24:269
15. Curti BD, Smith JW II (1995) Interleukin-1 in the treatment of cancer. Pharmacol Ther 65:291
16. de Kossodo S, Moore E, Gschmeissner S, East N, Upton C, Balkwill FR (1995) Changes in endogenous cytokines, adhesion molecules and platelets during cytokine-induced tumour necrosis. Br J Cancer 72:1165
17. Devore RF, Hellerqvist CG, Wakefield GB, Wamil BD, Thurman GB, Minton PA, Sundell HW, Yan HP, Carter CE, Wang YF, York GE, Zhang MH, Johnson DH (1997) Phase I study of the antineovascularization drug CM101. Clin Cancer Res 3:365
18. Eggermont AMM, Koops HS, Klausner JM, Kroon BBR, Schlag PM, Lienard D, van Geel AN, Hoekstra HJ, Meller I, Nieweg OE, Kettelhack C, Ben-Ari G, Pector J-C, Lejeune FJ (1996) Isolated limb perfusion with tumor necrosis factor and melphalan for limb salvage in 186 patients with locally advanced soft tissue extremity sarcomas. Ann Surg 224:756
19. Eggermont AMM, Koops HS, Klausner JM, Lienard D, Kroon BBR, Schlag PM, Ben-Ari G, Lejeune FJ (1997) Isolation limb perfusion with tumor necrosis factor alpha and chemotherapy for advanced extremity soft tissue sarcomas. Semin Oncol 24:547
20. Erkmen K, Egorin MJ, Reyno LM, Morgan R Jr, Doroshow JH (1995) Effects of storage on the binding of carboplatin to plasma proteins. Cancer Chemother Pharmacol 35:254
21. Flower MA, Zweit J, Hall AD, Burke D, Davies MM, Dworkin MJ, Young HE, Mundy J, Ott RJ, McCready VR, Carnochan P, Allen-Mersh TG (2001) 62Cu-PTSM and PET used for the assessment of angiotensin II-induced blood flow changes in patients with colorectal liver metastases. Eur J Nucl Med 28:99
22. Folkman J (1995) Clinical applications of research on angiogenesis. N Engl J Med 333:1757
23. Frackowiak RSJ, Lenzi G-L, Jones T, Heather JD (1980) Quantitative measurement of regional cerebral blood flow and oxygen metabolism in man using ^{15}O and positron emission tomography: theory, procedure, and normal values. J Comput Assist Tomogr 4:727
24. Gamble JR, Harlan JM, Klebanoff SJ, Vadas MA (1985) Stimulation of the adherence of neutrophils to umbilical vein endothelium by human recombinant tumor necrosis factor. Proc Natl Acad Sci U S A 82:8667
25. Hanan SH, Dookeran KA, Rao U, Rubin JT, Logan T (1997) Recombinant human TNF alpha produces neutrophil nadir in peripheral blood and hemorrhagic necrosis in syngenic murine breast carcinoma model. Proc Am Assoc Cancer Res 38:272
26. Herman WH, Holcomb JM, Hricik DE, Simonson MS (1999) Interleukin-1β induces endothelin-1 gene by multiple mechanisms. Transplant Proc 31:1412
27. Herrero P, Markham J, Bergmann SR (1989) Quantitation of myocardial blood flow with $H_2{}^{15}O$ and positron emission tomography: assessment and error analysis of a mathematical approach. J Comput Assist Tomogr 13:862
28. Herscovitch P, Markham J, Raichle ME (1983) Brain blood flow measured with intravenous $H_2{}^{15}O$. I. Theory and error analysis. J Nucl Med 24:782
29. Ito M, Lammertsma AA, Wise RJS, Bernardi S, Frackowiak RSJ, Heather JD, McKenzie CG, Thomas DGT, Jones T (1982) Measurement of regional cerebral blood flow and oxygen utilisation in patients with cerebral tumours using ^{15}O and positron emission tomography: analytical techniques and preliminary results. Neuroradiology 23:63
30. Jain RK (1988) Determinants of tumor blood flow: a review. Cancer Res 48:2641
31. Jia SF, Zwelling LA, Kleinerman ES (1995) Antitumor effect of IL-1 alpha and VP-16, ADR, mAMSA, VLB, TPT, cDDP against osteosarcoma cells. Proc Am Assoc Cancer Res 36:2857
32. Johnson CS, Chang MJ, Yu WD, Modzelewski RA, Grandis JR, Vlock DR, Furmanski P (1993) Synergistic enhancement by interleukin-1 alpha of cisplatin-mediated antitumor activity in RIF-1 tumor-bearing C3H/HeJ mice. Cancer Chemother Pharmacol 32:339
33. Kopp WC, Urba WJ, Rager HC, Alvord G, et al (1996) Induction of interleukin-1 receptor antagonist after interleukin-1 therapy in patients with cancer. Clin Cancer Res 2:501
34. Lienard D, Ewalenko P, Delmotte JJ, Renard N, Lejeune FJ (1992) High-dose recombinant tumor necrosis factor alpha in combination with interferon gamma and melphalan in isolation perfusion of the limbs for melanoma and sarcoma. J Clin Oncol 10:52
36. Logan TF, Kaplan SS, Bryant JL, Ernstoff MS, Krause JR, Kirkwood JM (1991) Granulocytopenia in cancer patients treated in a phase I trial with recombinant human tumor necrosis factor (TNF). J Immunother 10:84
35. Logan T, Gooding W, Carlos T, Kaplan S, Kirkwood J, Shipe-Spotloe J, Tompkins C, Donnelly S (1996) TNF induced granulocytopenia is associated with integrin upregulation on circulating cells in human cancer patients. Proc Am Assoc Cancer Res 37:3064
37. Mintun MA, Ter-Pogossian MM, Green MA, Lich LL, Schuster DP (1986) Quantitative measurement of regional pulmonary blood flow with positron emission tomography. J Appl Physiol 61:317
38. Murray JC (1992) Vascular damage and tumour response. Eur J Cancer 28A:1593
39. Nakatsumi Y, Shibata K, Bando T, Kassahara K, Fujimura M, Yoshida T, Okumura K, Matsuda T (1995) Enhanced antitumor effect of interleukin-1 beta (IL-1 beta) combined with etoposide (ET) on murine tumors. Proc Am Assoc Cancer Res 36:2796
40. Nemunaitis J, Buckner CC, Press O, Lilleby K, Buhles B, Singer J (1991) Phase I trial with interleukin-1α (IL-1α) in patients undergoing autologous bone marrow transplantation (ABMT) for acute myelogenous leukemia (AML). Blood 78:8a
41. Price P (1997) Is there a future for PET in oncology? Eur J Nucl Med 24:587

42. Ran S, Gao B, Duffy S, Watkins L, Rote N, Thorpe PE (1998) Infarction of solid Hodgkin's tumors in mice by antibody-directed targeting of tissue factor to tumor vasculature. Cancer Res 58:4646
43. Renard N, Lienard D, Lespagnard L, Eggermont A, Heimann R, Lejeune F (1994) Early endothelium activation and polymorphonuclear cell invasion precede specific necrosis of human melanoma and sarcoma treated by intravascular high-dose tumour necrosis factor alpha (RTNFα). Int J Cancer 57:656
44. Rhodes CG, Wise RJS, Gibbs JM, Frackowiak RSJ, Hatazawa J, Palmer AJ, Thomas DGT, Jones T (1983) In vivo disturbance of the oxidative metabolism of glucose in human cerebral gliomas. Ann Neurol 14:614
45. Robertson PA, Ross HJ, Figlin RA (1989) Tumor necrosis factor induces hemorrhagic necrosis of a sarcoma. Ann Intern Med 111:682
46. Rocci ML, Jusko WJ (1983) LAGRAN program for area and moments in pharmacokinetic analysis. Comput Prog Biomed 16:203
47. Sagar SM, Klassen GA, Barclay KD, Aldrich JE (1983) Antitumor treatment. Tumour blood flow: measurement and manipulation for therapeutic gain. Cancer Treat Rev 19:299
48. Saleem A, Harte RJ, Matthews JC, Osman S, Brady F, Luthra SK, Brown GD, Bleehen N, Connors T, Jones T, Price PM, Aboagye EO (2001) Pharmacokinetic evaluation of N-[2-(dimethylamino)ethyl]acridine-4- carboxamide in patients by positron emission tomography. J Clin Oncol 19:1421
49. Sekida T, Matsui T, Matsugi W, Warashina H, Ikeda Y, Ohashi M (1997) A novel antitumor agent: tumor blood flow inhibitor, KB-R8498 (abstract 1465). Proc Am Assoc Cancer Res 38:217
50. Skillings J, Wierzbicki R, Eisenhauer E, Venner P, Letendre F, Stewart D, Weinerman BA (1992) Phase II study of recombinant tumor necrosis factor in renal cell carcinoma: a study of National Cancer Institute of Canada Clinical Trials Group. J Immunother 11:67
52. Smith JW, Urba WJ, Curti BD, Elwood LJ, Steis RG, Janik JE, Sharfman WH, Miller LL, Fenton RG, Conlon KC, Sznol M, Creekmore SP, Wells NF, Ruscetti FW, Keller JR, Hestdal K, Shimizu M, Rossio J, Alvord WG, Oppenheim JJ, Longo DL (1992) The toxic and hematologic effects of interleukin-1 alpha administered in a phase I trial to patients with advanced malignancies. J Clin Oncol 10:1141
51. Smith JW II, Longo DL, Alvord WG, Janik JE, Sharfman WH, Gause BL, Curti BD, Creekmore SP, Holmlund JT, Fenton RG, Sznol M, Miller LL, Shimizu M, Opppenheim JJ, Fiem SJ, Hursey JC, Powers GC, Urba WJ (1993) The effects of treatment with interleukin-1α on platelet recovery after high-dose carboplatin. N Engl J Med 328:756
53. Twining SS, Wilson PM, Ngamkitichakul C (1999) Extrahepatic synthesis of plasminogen in the human cornea is up-regulated by interleukins-1α and -1β. Biochem J 339:705
54. Usui N, Matsushima K, Pilaro AM, Longo DL, Wiltrout RH (1996) Antitumor effects of human recombinant interleukin-1 alpha and etoposide against human tumor cells: mechanism for synergism in vitro and activity in vivo. Biotherapy 9:199
55. Veltri S, Smith JW II (1996) Interleukin 1 trials in cancer patients: a review of the toxicity, antitumor and hematopoietic effects. Stem Cells 14:164
56. Verschraegen CF, Kudelka AP, Termrungruanglert W, de Leon CG, Edwards CL, Freedman RS, Kavanagh JJ, Vadhan-Raj S (1996) Effects of interleukin-1 alpha on ovarian carcinoma in patients with recurrent disease. Eur J Cancer 32A:1609
57. Wahl RL (1997) Clinical oncology update: the emerging role of positron emission tomography: part I. PPO Updates 11:1
58. Wang Z, Lee KB, Reed E, Sinha BK (1996) Sensitization by interleukin-1α of carboplatinum anti-tumor activity against human ovarian (NIH:OVCAR-3) carcinoma cells in vitro and in vivo. Int J Cancer 67:583
59. Warnke PC, Berlis A, Weyerbrock A, Ostertag CB (1997) Effect of LINAC radiosurgery on regional cerebral blood flow, glucose metabolism and sodium-potassium ATPase in skull base meningiomas and metastasis. Acta Neurochir 68:124
60. Wilson CBJH, Lammertsma AA, McKenzie CG, Sikora K, Jones T (1992) Measurements of blood flow and exchanging water space in breast tumors using positron emission tomography: a rapid and noninvasive dynamic method. Cancer Res 52:1592
61. Wilson WH, Bryant G, Jain W, Smith J, Fox M, Miller L, Goldspiel B, Tannenbaum S, Cowen K, Wittes R (1992) Phase I study of infusional interleukin-1α (IL-1) with ifosfamide (I), CBDCA (C), and etoposide (E) (ICE) and autologous bone marrow transplant (BMT). Proc Am Soc Clin Oncol 11:335
62. Worth LL, Jaffe N, Benjamin RS, Papadopoulos NE, Patel S, Raymond AK, Jia SF, Rodriguez C, Gano J, Gianan MA, Kleinerman ES (1997) Phase II study of recombinant interleukin 1alpha and etoposide in patients with relapsed osteosarcoma. Clin Cancer Res 3:1721
63. Yeh KC, Kwan KC (1978) A comparison of numerical integrating algorithms by trapezoidal, LaGrange and spline approximation. J Pharmacokinet Biopharm 6:79
64. Ziegler SI, Haberkorn U, Byrne H, Tong C, Schosser R, Krieter H, Kaja S, Richolt JA, Lammertsma AA, Price P (1996) Measurement of liver blood flow using oxygen-15 labelled water and dynamic positron emission tomography: limitations of model description. Eur J Nucl Med 23:169